Plant, Cell & Environment

Plant, Cell and Environment (2010) doi: 10.1111/j.1365-3040.2010.02251.x

Plasma membrane Ca^{2+} transporters mediate virus-induced acquired resistance to oxidative stress

SERGEY SHABALA[1], LONE BÆKGAARD[2], LANA SHABALA[3], ANJA FUGLSANG[2], OLGA BABOURINA[4], MICHAEL G. PALMGREN[2], TRACEY A. CUIN[1], ZED RENGEL[4] & LEV G. NEMCHINOV[5]

[1]School of Agricultural Science and [3]NeuroRepair Group, Menzies Research Institute, University of Tasmania, Private Bag 54, Hobart, Tas 7001, Australia, [2]Centre for Membrane Pumps in Cells and Disease – PUMPKIN, Danish National Research Foundation, Department of Plant Biology and Biotechnology, Faculty of Life Sciences, University of Copenhagen, Thorvaldsensvej 40, DK-1871 Frederiksberg C, Denmark, [4]School of Earth and Environment, The University of Western Australia, Crawley, West Australia 6009, Australia and [5]USDA/ARS, Plant Sciences Institute, Molecular Plant Pathology Laboratory, Beltsville, Maryland 20705, USA

ABSTRACT

This paper reports the phenomenon of acquired cross-tolerance to oxidative stress in plants and investigates the activity of specific Ca^{2+} transport systems mediating this phenomenon. *Nicotiana benthamiana* plants were infected with *Potato virus X* (PVX) and exposed to oxidative [either ultraviolet (UV-C) or H_2O_2] stress. Plant adaptive responses were assessed by the combined application of a range of electrophysiological (non-invasive microelectrode ion flux measurements), biochemical (Ca^{2+}- and H^+-ATPase activity), imaging (fluorescence lifetime imaging measurements of changes in intracellular Ca^{2+} concentrations), pharmacological and cytological transmission electrone microscopy techniques. Virus-infected plants had a better ability to control UV-induced elevations in cytosolic-free Ca^{2+} and prevent structural and functional damage of chloroplasts. Taken together, our results suggest a high degree of crosstalk between UV and pathogen-induced oxidative stresses, and highlight the crucial role of Ca^{2+} efflux systems in acquired resistance to oxidative stress in plants.

Key-words: Ca^{2+}/H^+ exchanger; Ca^{2+}-pump; chloroplast; mesophyll; potato virus X; UV irradiation.

INTRODUCTION

Cross-tolerance is the synergistic co-activation of non-specific stress-responsive pathways, referring to a situation when an organism's exposure to one stress increases its tolerance to another (Sabehat, Weiss & Lurie 1998; Mittler 2006). This cross-tolerance can often go through biotic-abiotic stress boundaries (Bowler & Fluhr 2000; Bostock 2005). Increased salinity tolerance was reported in tomato plants in response to wounding (Capiati, Pais & Tellez-Inon 2006). Exposure of tobacco plants to ultraviolet (UV)-C increased resistance to tobacco mosaic virus (Yalpani *et al.* 1994), and ozone treatment of *Arabidopsis thaliana* causes induced resistance to *Pseudomonas syringae* (Sharma *et al.* 1996). A crosstalk between pathogen infection and salinity and oxidative stress in tomato was shown in a more recent work by AbuQamar *et al.* (2009).

In most cases, induced cross-tolerance was attributed to reactive oxygen species (ROS) production during the so-called 'oxidative burst' – the rapid release of H_2O_2 – and is linked to plant responses to avirulent pathogens. It was previously suggested that relatively low levels of ROS can be used as signalling molecules to control abiotic stress responses and this was responsible for modulation of various cellular functions (Remacle *et al.* 1995; Pang & Wang 2008). ROS may also serve as messengers for the activation of defence genes (Dempsey, Shah & Klessig 1999). This assumes a broader role of ROS, in addition to their well-known toxic effects (Apel & Hirt 2004). Although the specific details of this control remain elusive, all researchers are unanimous that Ca^{2+} signalling plays a key role in this process.

The calcium ion is a ubiquitous signalling molecule in plants (Hepler & Wayne 1985; Hetherington & Brownlee 2004). An increase in cytosolic-free calcium, $[Ca^{2+}]_{cyt}$, couples a diverse array of signals and receptors. Numerous plant signal transduction pathways use Ca^{2+} as an integral signalling component (Sanders, Brownlee & Harper 1999).

Calcium fluxes are among the earliest responses to pathogen invasion. Elicitor-induced elevations in $[Ca^{2+}]_{cyt}$ were reported during hypersensitive plant–pathogen interactions (Nürnberger *et al.* 1994; Blume *et al.* 2000; Lecourieux *et al.* 2002); these are believed to be essential for the development of the oxidative burst needed to trigger the activation of several plant defence reactions (Blumwald, Aharon & Lam 1998; Lecourieux *et al.* 2002). On the other hand, numerous reports of oxidative stress-induced elevation in $[Ca^{2+}]_{cyt}$ are available in the literature (e.g. Pei *et al.* 2000; Romani *et al.* 2004; Hu *et al.* 2007) and plasma membrane Ca^{2+}-permeable channels have been shown to play a critical role in oxidative stress signalling (Pei *et al.* 2000; Demidchik *et al.* 2003; Mori & Schroeder 2004). Taken together, these results suggest that interactions between calcium

Correspondence: S. Shabala. Fax: +613 62262642; e-mail: sergey.shabala@utas.edu.au

metabolism and ROS may be crucial for controlling cross-tolerance at the cellular level (Bowler & Fluhr 2000).

Although transient increases in $[Ca^{2+}]_{cyt}$ are essential for plant responses to a variety of environmental stimuli, long-lasting elevations in $[Ca^{2+}]_{cyt}$ are harmful for cells. Hence, the basal conditions must be restored back to resting level after the signal is completed, enabling cells to react to further signals (Sanders *et al*. 1999; Beffagna, Buffoli & Busi 2005). This subsequent re-establishment of $[Ca^{2+}]_{cyt}$ to resting levels is achieved by active Ca^{2+} transport systems such as Ca^{2+} pumps and Ca^{2+}/H^+ antiporters (Sanders *et al*. 1999; White & Broadley 2003).

In animal systems, active Ca^{2+} efflux systems have been widely implicated in oxidative stress responses (Jornot *et al*. 1999; Zaidi & Michaelis 1999). However, surprisingly little is known about the involvement of Ca^{2+} efflux systems in oxidative stress responses in plant cells. Earlier, Romani *et al*. (2004) showed that submicromolar concentrations of eosin yellow (EY; a P_{2B}-type Ca^{2+}-ATPase inhibitor) prevented both the increase in Ca^{2+} efflux and the transient ROS accumulation in *Egeria densa* in response to abscisic acid treatment. This result was explained by assuming an important role of plasma membrane Ca^{2+}-ATPase in switching off the signal triggering ROS production. Another report from the same group implicated plasma membrane Ca^{2+}-ATPase activation in plant adaptation to osmotic stress (Beffagna *et al*. 2005). Recently, an important role of Ca^{2+} efflux system in tobacco hypersensitive response to *P. syringae* was established (Nemchinov, Shabala & Shabala 2008).

This paper investigates the role and specific identity of transport systems mediating increased oxidative (UV-C) stress tolerance acquired by *Nicotiana benthamiana* plants infected with *potato virus X* (PVX). We show that virus-infected plants have a superior ability to control UV-induced elevations in cytosolic-free Ca^{2+} and prevent structural damage of chloroplasts. We also provide evidence for the critical role of plasma membrane Ca^{2+} efflux systems in this process.

MATERIALS AND METHODS

Plant material

Tobacco (*N. benthamiana* L.) plants were grown from seeds in 2 L pots in a standard potting mix (Chen *et al*. 2005) at 25 °C with a 16 h light period in the containment greenhouse facilities at United States Department of Agriculture (USDA)/Agricultural Research Services (ARS), Beltsville, MD (USA), at the University of Tasmania (Hobart, Australia) glasshouse, or at the Department of Plant Biology and Biotechnology, University of Copenhagen (Denmark). Fully developed 6- to 8-week-old excised leaves were used for measurements.

Transcript preparation and inoculation of plants

PVX-based vector pP2C2S (a kind gift from D. Baulcombe, Sainsbury Laboratory, Norwich, UK) incorporates a bacteriophage T7 RNA polymerase promoter upstream from the viral cDNA, which expedites production of infectious viral transcripts. PVX plasmids were linearized with restriction enzyme Spe I before the transcription, and capped transcripts were generated *in vitro* from ~ 1 μg of DNA template using Ambion's T7 mMessage Machine kit (Ambion, Austin, TX, USA) according to the manufacturer's instructions. The transcription reaction was incubated at 37 °C for 2 h and aliquots were evaluated on a 0.8% agarose gel. Entire undiluted transcription reactions (approximately 20–30 μg of RNA in 20 μL of reaction buffer) were mechanically rub inoculated onto fully expanded three top leaves of 3-week-old *N. benthamiana* plants dusted with carborundum. Mock controls were prepared at the same time by infiltrating leaves with the buffer. Plants were grown for a further 3–4 weeks (as described above) before measurements were taken.

Sample isolation and UV-light treatments

Fully developed leaves were excised from either mock controls or PVX-inoculated plants and brought in the lab in sealed plastic bags. For electrophysiological and transmission electrone microscopy micrographs, the leaf epidermis was gently removed with fine forceps, and mesophyll segments of about 4×5 mm size were cut and left floating (peeled side down) on a surface of the basic salt media (BSM) solution (0.1 mM $CaCl_2$ + 0.2 mM KCl; pH 5.5 unbuffered) as described elsewhere (Shabala, Babourina & Newman 2000; Shabala *et al*. 2007) for about 3 h. At this time, Petri dishes with floating mesophyll segments were placed into HL-2000 Hybrilinker System (UVP, LLC, Upland, CA, USA) and exposed to UV-C treatment (254 nm; 0.1 J cm^{-2}) for various lengths of time (10 to 150 min). Net Ca^{2+} fluxes were measured either immediately (within 1–1.5 min) or 2 hours after UV-C exposure.

In chlorophyll fluorescence experiments, leaf segments of ~ 20×20 mm, with the epidermis still attached, were cut from excised leaves and left floating on the surface of a small (35 mm diameter) Petri dish containing 5 mL of BSM solution. The segments were exposed to UV-C (as above) for various lengths of time, from 10 min to 12 h. Leaf segments were removed from the UV incubator, and left under normal laboratory conditions for 2 h (still in the BSM solution). Chlorophyll fluorescence characteristics (F_o, F_m and F_v/F_m) were then measured using an OS-500 PAM fluorometer (Opti-Sciences, Tyingsborro, MA, USA).

For biochemical analysis (ATPase assays), 15–20 g leaf material was treated with either 0.1 or 1 J cm^{-2} UV-C light (Bio-Link crosslinker, Vilber Lourmat, Cedex 1, France) for 20 min while floating on MilliQ water and further left on the table for 2 h at room temperature. As control, leaves floating on MilliQ water were left on the table for 2 h and 20 min at room temperature before membrane purification.

Non-invasive ion flux measurements

Net Ca^{2+} and K^+ fluxes were measured non-invasively using the microelectrode ion flux measuring technique (MIFE;

UTAS Innovation Ltd, Hobart, Tasmania, Australia). All details on microelectrode fabrication and calibration are given elsewhere (Shabala & Newman 2000; Shabala *et al*. 2006b).

Appropriately treated mesophyll segments were immobilized in a Perspex holder and placed in a measuring chamber. Electrode tips were positioned 50 μm above the leaf surface under dim (20 μmol s^{-1} m^{-2}) microscopic light. During measurement, electrodes were moved back and forth in a square-wave manner by a computerized stepper motor between two positions (50 and 120 μm above the leaf surface) with 0.125 Hz frequency. Net ion fluxes were calculated from measured differences in the electrochemical potential between these two positions for each ion as described earlier (Shabala *et al*. 2006a). Light treatment was given using bright (2500 μmol s^{-1} m^{-2}) white light regimes from inverted microscope (model RTC-6; Radical Instruments, Ambala Cantt, India).

Tissue preparation for transmission electron microscope

Leaf tissues were fixed for 2 h at room temperature by immersion in 2.5% glutaraldehyde/0.05 M NaCacodylate buffer, pH 7.0 and then placed into a refrigerator at 4 °C degrees overnight. This was followed by washing in a NaCacodylate buffer rinse, six times over 1 h, post-fixed in 2% buffered osmium tetroxide for 2 h, dehydrated in EtOH and infiltrated with Spurr's low-viscosity embedding resin. Furthermore, 60–90 nm silver–gold sections of the tissue were cut on a Reichert/AO Ultracut microtome with a Diatome diamond knife and mounted onto 400 mesh Ni grids. They were stained with 4% uranyl acetate and 3% lead citrate and viewed in a Hitachi H-7000 microscope at 75 kV.

Conventional confocal and fluorescence lifetime imaging measurements

Calcium GreenTM AM (Ca-Green-AM, Molecular Probes, Eugene, OR, USA) was used to quantify cytosolic-free Ca^{2+} levels in control and PVX-inoculated plants before and after UV-C exposure. All details on dye loading, fluorescence lifetime imaging (FLIM) calibration and measurements and data analysis are available in our previous publication (Guo, Babourina & Rengel 2009).

Pharmacology

Leaf mesophyll segments were pre-treated in a range of known Ca^{2+} channels and Ca^{2+} ATPase blockers for 1 h prior to UV exposure. The following chemicals were used: La^{3+} ($LaCl_3$; 1 mM), Gd^{3+} ($GdCl_3$; 50 μM), EY (0.5 μM) and erythrosine B (EB; 2 to 10 μM).

Isolation of plasma membranes

Plasma membranes were isolated from tobacco leaves by aqueous two-phase partitioning as previously described (Larsson, Widell & Kjellbom 1987) with minor modifications (Chen *et al*. 2007a). Between 15 and 20 g of tobacco leaves were homogenized on ice in 70 mL homogenization buffer [50 mM 3-morpholino-propanesulfonic acid, 5 mM ethylenediaminetetraacetic acid (EDTA), 0.33 M sucrose, 0.6% polyvinylpyrrolidione, 5 mM ascorbate, 5 mM dithiothreitol (DTT) and 1 mM phenylmethylsulfonyl fluoride (PMSF)], phosphatase inhibitors (25 mM NaF, 1 mM NaMo, 50 mM Na pyrophosphate) and pH adjusted to 7.5. Plasma membrane fractions were isolated and resuspended in a buffer containing 0.25 M sucrose, 10 mM Bis-Tris propane-4-(2-hydroxyethyl)-1-piperazineethanesulfonic acid, pH 7.5, 50 mM KCl, 1 mM EDTA, 1 mM DTT and 1 mM PMSF. The protein concentrations were determined according to Bradford (1976) using γ-globulin as a protein standard. The membranes were frozen in liquid N_2 and stored at –80 °C.

ATPase assay

ATPase activity was determined as described in our previous publication (Bækgaard *et al*. 2006). Five micrograms of membrane proteins in resuspension buffer were incubated for 45 min at 25 °C in four buffers: (1) EGTA (no free Ca^{2+}); (2) Ca (estimated free Ca^{2+} concentration of 70 μM); (3) CaM (20 μg mL^{-1} bovine brain; Sigma, St Louis, MO, USA); and (4) Ca/CaM (70 μM-free Ca^{2+} plus 20 μg mL^{-1} CaM). Free Ca^{2+} concentrations were calculated using WEBMAXCLITE 1.15 software (maxchelator.stanford.edu; Patton, Thompson & Epel 2004).

Measurement of proton transport by the plasma membrane H^+-ATPase

Proton transport was assayed as described previously (Niittyla *et al*. 2007) by monitoring fluorescence quenching of 9-amino-6-chloro-2-methoxyacridine, a dye that upon protonation accumulates inside vesicles in an impermeant form. The initial decrease in fluorescence correlates with the amount of protons transported into plasma membrane vesicles by the H^+-ATPase.

Protein immunodetection and CaM overlay assay

Expression levels and CaM binding of P_{2B} Ca^{2+}-ATPases in plasma membrane fractions were analysed by Western blotting and CaM overlay assays, respectively. Forty micrograms membrane proteins were precipitated with trichloroacetic acid, separated by sodium dodecyl sulphate–polyacrylamide gel electrophoresis (Laemmli 1970) and immobilized on polyvinylidine difluoride membrane (Millipore, Billerica, MA, USA). Immunodetection of P_{2B} Ca^{2+}-ATPases was performed using a non-isoform-specific polyclonal antibody for P_{2B} Ca^{2+}-ATPases with the sequence: SDYRQSLQFRDLDRE (the antibody was a kind gift from Prof M. Maeshima, Univ. Nagoya, Japan). Bands were visualized with the 5-bromo-4-chloro-3-indolyl

phosphate/nitroblue tetrazolium colour development substrate (Promega, Madison, WI, USA). CaM binding to P_{2B} Ca^{2+}-ATPases was determined by CaM overlay assays carried out as previously described (Schiøtt *et al*. 2004).

14-3-3 overlay assays were performed as described previously (Fuglsang *et al*. 1999). Briefly, equal amounts of plasma membrane protein were loaded on a regular sodium dodecyl sulphate gel, blotted to a nitrocellulose membrane and incubated with MRGSH6-tagged GF14-14-3-3 protein. Bound 14-3-3 protein was subsequently detected immunologically using a primary anti-RGSH6 antibody (Qiagen, Valencia, CA, USA) followed by incubation with a secondary anti-IgG antibody conjugated with alkaline phosphatase. For detection of H^+-ATPase, antibodies raised against the C terminus (number 759) of plasma membrane H^+-ATPase were used (1:5000).

RESULTS

PVX-infected plants show better tolerance to UV stress

Symptoms indicative of typical PVX infection on *N. benthamiana* were first visible as distinct vein clearing 5–7 d post-inoculation (dpi). Plants eventually became systemically infected and developed characteristic PVX symptoms including vein clearing, green mosaic and general stunting appearance within 10–14 dpi (Supporting Information Fig. S1b). Over the next 15–20 d, they appeared to recover, with no major difference observed in growth rate or shoot biomass (Supporting Information Fig. S1d = 25 d after inoculation; Supporting Information Fig. S1c = mock control). At this stage, fully developed systemic leaves from the PVX-infected plants as well as leaves similar in size from mock controls were excised and exposed to various doses of UV-C (254 nm; 0.1 J cm^{-2}; duration from 10 min to 12 h). Chlorophyll fluorescence measurements were used to assess the magnitude of UV stress damage to leaf photosynthetic machinery. Increased UV exposure caused a very substantial and progressive decline in the maximal photochemical efficiency of photosystem II (PSII) (estimated as F_v/F_m ratio) in both mock control and PVX-inoculated leaves (Fig. 1). However, for most UV treatments, the UV stress-induced decline in the F_v/F_m ratio was significantly ($P < 0.05$) smaller in PVX-inoculated leaves compared with the control, indicating less functional damage to PSII. To a large extent, this reduction could be explained by the greater UV damage to chloroplast structure in non-inoculated leaves (Fig. 2). No substantial difference in the chloroplast structure was observed between mock controls and PVX-infected plants in the absence of UV stress (Fig. 2; panels a and b, respectively). Increasing doses of UV radiation progressively affected the regular pattern and shape of thylakoids in control plants, reducing the number of starch grains and increasing the amount of spherical electron-dense granules. Chloroplasts looked swollen, with their outer membrane often broken (Fig. 2c,e). These damaging effects of UV light were less pronounced in PVX-inoculated leaves (Fig. 2d,f), with 20 min of UV-C treatment causing no visible damage to chloroplast structure (Fig. 2d).

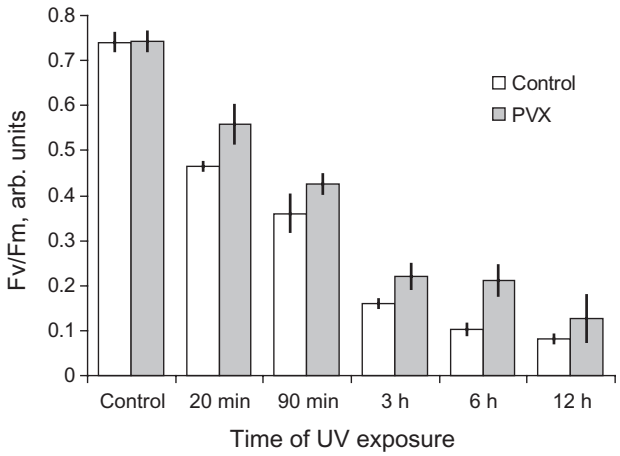

Figure 1. Maximal photochemical efficiency of photosystem II (chlorophyll fluorescence F_v/F_m value) of mock controls and potato virus X (PVX)-inoculated leaves exposed to various doses of ultraviolet (UV)-C radiation. Mean ± SE ($n = 6$ to 20).

PVX-infected plants show better tolerance to H_2O_2 treatment

Further experiments were conducted comparing responses from mock control and PVX-inoculated mesophyll tissues in response to acute and prolonged H_2O_2 treatments. Similar to previously published reports on *Arabidopsis* (Demidchik, Shabala & Davies 2007), acute 5 mM H_2O_2 treatment has triggered a significant net Ca^{2+} uptake into tobacco mesophyll cells (Fig. 3a). Peak net Ca^{2+} influx was twofold higher in mock controls (57 ± 6.2 nmol m^{-2} s^{-1}) compared with PVX-inoculated segments (27 ± 5.1 nmol m^{-2} s^{-1}) (significant at $P < 0.05$). At the same time, acute H_2O_2 stress also caused a pronounced K^+ efflux from mesophyll cells (Fig. 3b); an efflux that was significantly (at $P < 0.05$) higher in mock controls compared with PVX-inoculated samples (111 ± 6.4 versus 79 ± 4.9 nmol m^{-2} s^{-1}). Similar results were obtained for prolonged oxidative stress treatment (24 h of 0.5 mM H_2O_2). PVX-inoculated leaves were actively pumping Ca^{2+} out (net efflux), while mock controls were still taking up Ca^{2+}. Potassium 'leak' from the cell was also much (significant at $P < 0.05$) attenuated in PVX-inoculated leaves (Fig. 3c).

Cytosolic Ca^{2+} levels are lower in PVX inoculated plants under oxidative stress conditions

To quantify the effects of PVX inoculation and UV-C exposure on cytosolic Ca^{2+} concentrations, $[Ca^{2+}]_{cyt}$, in tobacco leaf mesophyll, conventional confocal and FLIM measurements were undertaken. PVX-inoculated plants had

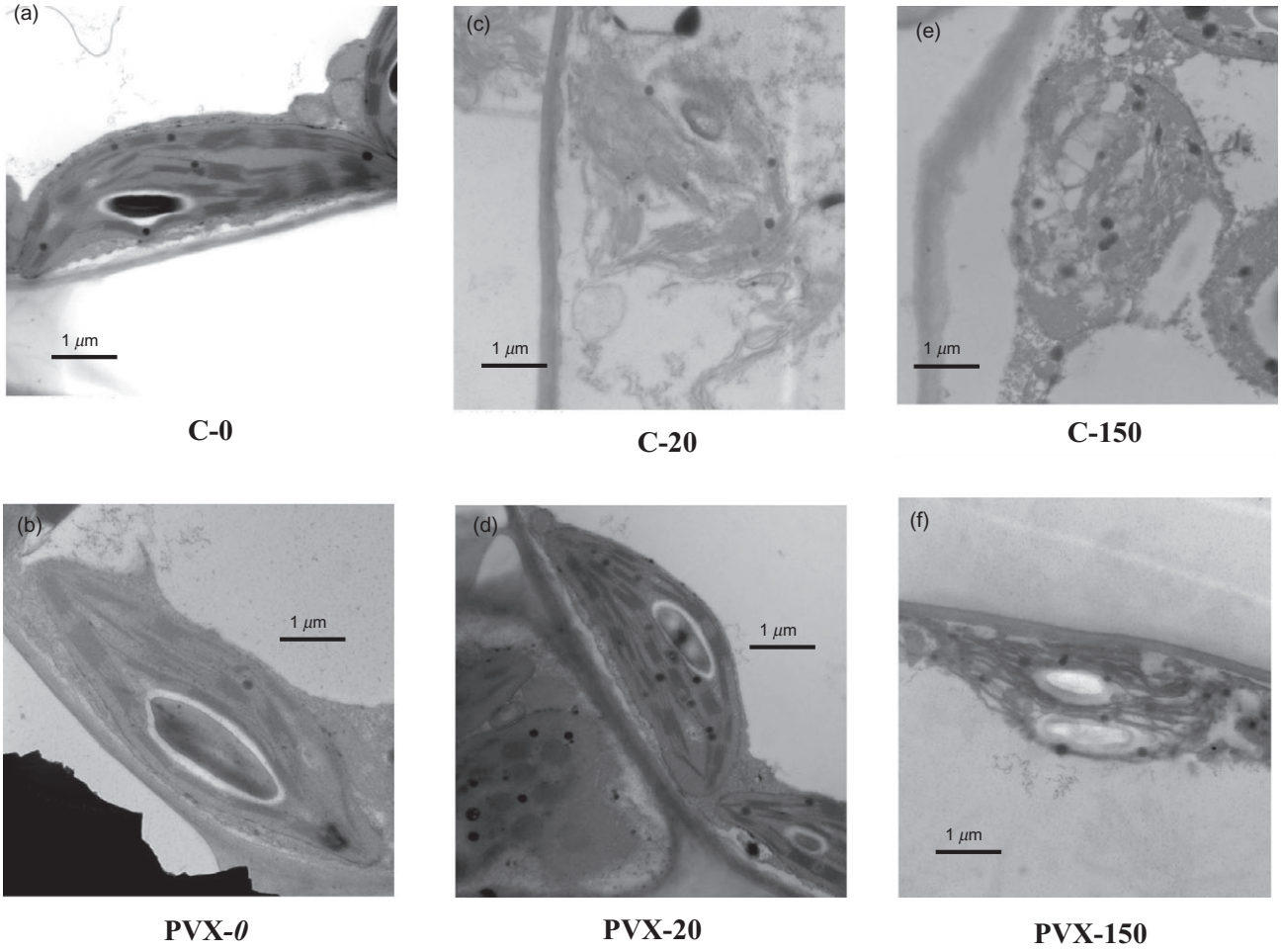

Figure 2. Ultrastructure of chloroplasts from leaf tissues irradiated with ultraviolet (UV)-C light. C – mock control (top row); potato virus X (PVX) – inoculated leaves (bottom row). The number after the code is duration of UV treatment in minutes (0, 20 and 150 min, respectively).

intrinsically lower $[Ca^{2+}]_{cyt}$ values compared with control (139 ± 9 and 209 ± 15 nM, respectively; significant at $P < 0.05$) (Fig. 4). Leaf exposure to UV-C caused a significant elevation in $[Ca^{2+}]_{cyt}$ in both control and PVC-inoculated plants. However, at all times, $[Ca^{2+}]_{cyt}$ values for PVX-inoculated plants were significantly lower than appropriate controls (Fig. 4).

Active plasma membrane Ca^{2+} transporters mediate plant adaptive responses to oxidative stress

To explain the above results and distinguish between active Ca^{2+} extrusion from the cell versus Ca^{2+} sequestration in organelles, net Ca^{2+} fluxes were measured non-invasively using the MIFE technique. Twenty minutes of UV-C treatment caused a dramatic increase in the magnitude of net Ca^{2+} uptake when measured immediately after UV stress (grey circles in Fig. 5a), especially under the light conditions. Two hours later, however, a significant ($P < 0.01$) net Ca^{2+} efflux was measured (grey triangles in Fig. 5a). As passive Ca^{2+} leak from the cytosol is thermodynamically impossible, such efflux cannot be attributed to the general change in plasma membrane permeability and may be explained *only* by the activation of some Ca^{2+} efflux (active) system at the plasma membrane (e.g. either Ca^{2+}-ATPases or Ca^{2+}/H^+ exchanger; White & Broadley 2003).

The kinetics of Ca^{2+} efflux was strikingly different between control- and PVX-inoculated leaves. Figure 5b shows two typical examples for each treatment immediately after 20 min of UV exposure. PVX-infected leaves (those presumably with acquired ROS tolerance) reverted to net Ca^{2+} efflux within a few minutes after UV treatment ceased, while for non-inoculated controls, it took much longer (*c*. 15 min) to switch from net Ca^{2+} uptake to Ca^{2+} efflux (Fig. 5b). This suggests that PVX-inoculated cells have much better capacity to activate plasma membrane Ca^{2+} efflux systems to deal with UV-induced elevation in cytosolic-free Ca^{2+} (Fig. 4), thereby preventing damage to chloroplast structure (Fig. 2).

Further evidence for the involvement of active Ca^{2+} transport systems was obtained from pharmacological

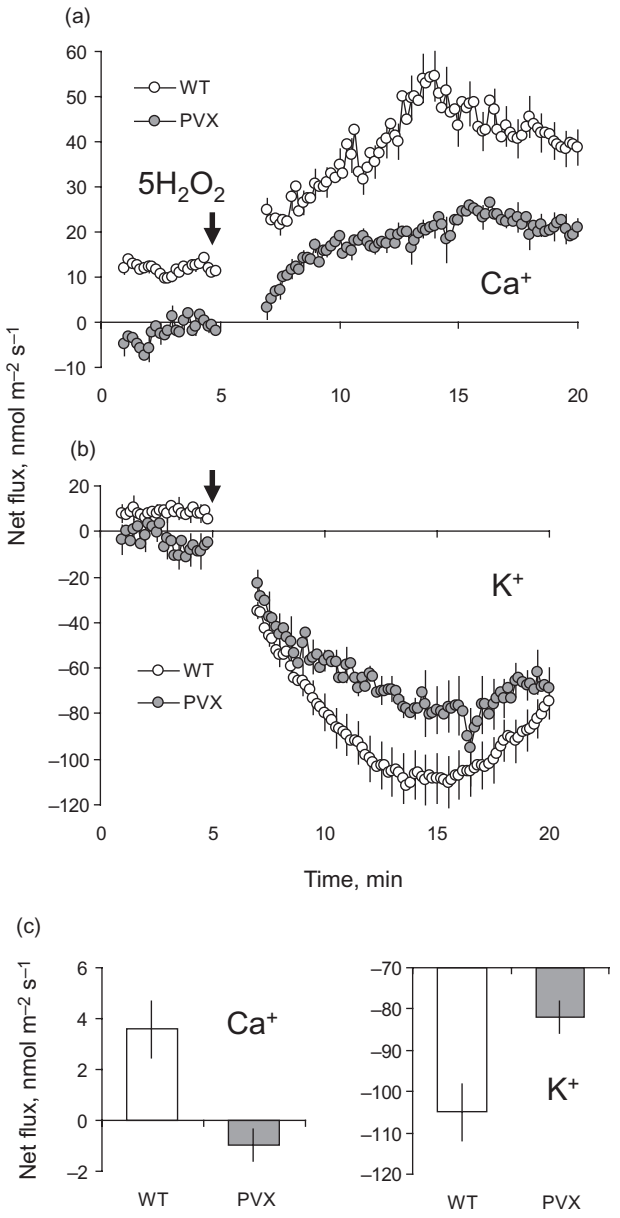

Figure 3. Evidence for increased oxidative stress tolerance in potato virus X (PVX)-inoculated leaves. Transient Ca^{2+} (a) and K^+ (b) flux kinetics from tobacco mesophyll cells in response to peroxide treatment (5 mM H_2O_2 added at 5 min) are shown. Mean ± SE ($n = 5$). Open symbols = WT (mock control); closed symbols = PVX-inoculated plants. (c) steady-state Ca^{2+} and K^+ fluxes from tobacco mesophyll cells after 24 h exposure to 0.5 mM H_2O_2. Mean ± SE ($n = 16$ to 30).

experiments. Application of La^{3+} and Gd^{3+}, two known blockers of Ca^{2+}-permeable plasma membrane channels, has resulted in a significant shift towards net Ca^{2+} efflux, both in the dark and under light conditions (Fig. 6). This further suggests that, under normal condition, channel-mediated Ca^{2+} uptake is balanced by the activity of some plasma membrane-based Ca^{2+} efflux system.

Plasma membrane Ca^{2+}/H^+ exchangers but not Ca^{2+}-ATPases mediate net Ca^{2+} efflux under oxidative stress conditions

To separate the different types of active Ca^{2+} transport systems, experiments were conducted using two specific inhibitors for P_{2B}-type Ca^{2+}-ATPases: EB (Bush 1995) and EY (Beffagna *et al.* 2005). Two hours of pre-treatment in

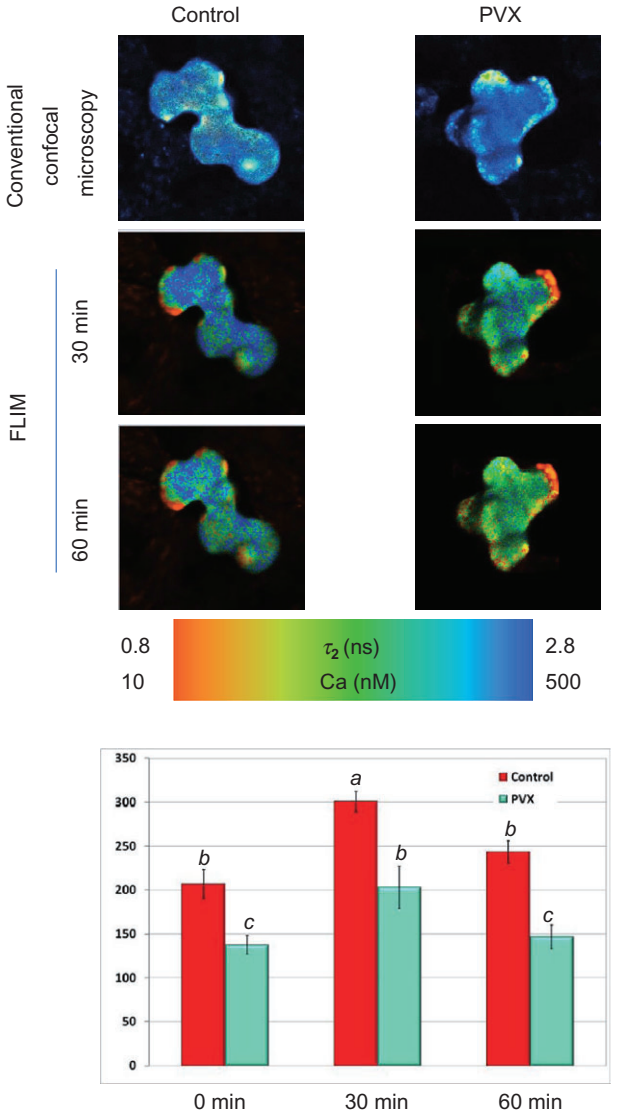

Figure 4. Intracellular Ca^{2+} concentration in mesophyll cells of control and potato virus X (PVX)-inoculated *Nicotiana benthamiana* plants assessed by fluorescence life-time imaging (FLIM) analysis. Leaf samples were exposed to ultraviolet (UV)-C treatment for 20 min, and FLIM images were taken 30 and 60 min after the UV exposure. The colour range in the pseudocoloured FLIM images is based on τ_2, lifetime of the long component, measured for Ca-Green assuming a double exponential decay for lifetime distribution for this dye. Values are means ± SE ($n = 5$–7). Statistical significance was estimated by analysis of variance. Different letters indicate significant differences at $P \leq 0.05$.

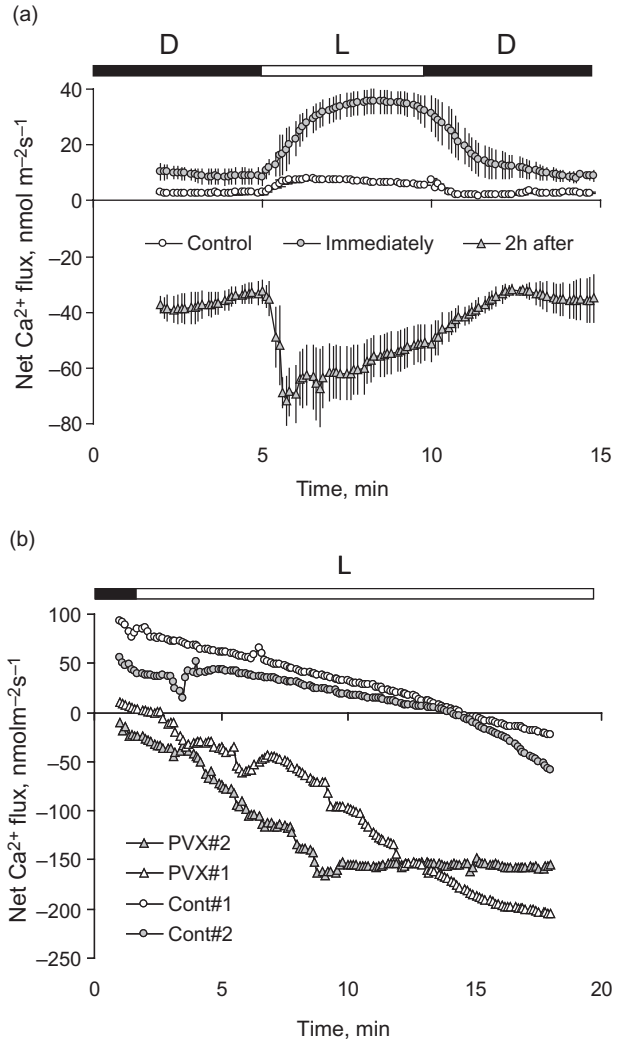

Figure 5. (a) Time dependence of net Ca^{2+} fluxes from tobacco mesophyll cells after ultraviolet (UV)-C exposure. Leaf samples were exposed to UV-C treatment for 20 min, and net Ca^{2+} fluxes were measured in response to dark/light fluctuations either immediately (within 1–2 min; closed circles) or 2 h after (closed triangles) after the end of UV treatment. Leaf segments not exposed to UV-C treatment were used as control (open circles). Mean ± SE ($n = 5$ to 8). (b) Kinetics of net Ca^{2+} fluxes measured from mock controls and potato virus X (PVX)-inoculated leaves immediately after 20 min exposure to UV-C treatment. Two typical examples for each treatment are shown. Note the time difference between treatments when net Ca^{2+} efflux becomes evident.

either of these inhibitors had no significant (at $P < 0.05$) impact on the magnitude of net Ca^{2+} fluxes from tobacco mesophyll segments compared with appropriate control (Fig. 6). This suggests that the plasma membrane Ca^{2+}-ATPases play a limited (if any) role in mediating Ca^{2+} efflux under oxidative stress conditions. This conclusion is further supported by measurements of Ca^{2+}-ATPase activity in purified plasma membrane vesicles from tobacco leaves (Fig. 7). These measurements were performed in four different buffers: (1) EGTA (no free Ca^{2+}); (2) Ca^{2+} (estimated free Ca^{2+} concentration of 70 μM); (3) CaM (20 μg mL^{-1}); and (4) Ca^{2+}/CaM (70 μM-free Ca^{2+} plus 20 μg mL^{-1} CaM). No significant (at $P < 0.05$) difference in Ca^{2+}-ATPase activity was found between these buffers for any of the four treatments used (mock control and PVX-inoculated leaves ± UV exposure) (Fig. 7). These findings were further supported by Western blot using an antibody known to recognize several P_{2B} Ca^{2+}-ATPases (CaM-stimulated types) in *Arabidopsis* (Fig. 8c). Polypeptides immunodecorated with this antibody corresponded in molecular mass to polypeptides decorated in the CaM overlay assay (8D). No noticeable difference was observed in expression levels of plasma membrane Ca^{2+}-ATPases or in their potency to bind CaM (Fig. 8c,d). An alternative active Ca^{2+} efflux system, which could be responsible for the observed net Ca^{2+} efflux shown in Figs 3 and 4, are plasma membrane Ca^{2+}/H^+ exchangers (Kasai & Muto 1990), a less defined system that is difficult to characterize due to the absence of pharmacological or molecular tools to detect them.

Plasma membrane H^+-ATPase-catalysed proton pumping increases in response to UV light and viral infection

The plasma membrane H^+-ATPase is an electrogenic proton pump responsible for extracellular acidification and establishment and maintenance of the membrane potential (Palmgren 2001). Proton pumping by plasma membrane H^+-ATPases is readily assayed by measuring intravesicular acidification of isolated plasma membrane vesicles in response to the addition of ATP. Plasma membrane vesicles isolated from plants pre-treated with UV light had an increase in ATP-dependent proton pumping of about 40% (Fig. 8a), whereas PVX inoculation gave rise to a slightly less potent increase (Fig. 8a). The effects of UV light and PVX inoculation were additive resulting in an approximately doubling of the proton pumping capacity of the vesicles (Fig. 8a). The amount of plasma membrane H^+-ATPase did not change accordingly to the three different treatments (Fig. 8e), nor did the amount of 14-3-3 protein, which is capable of interacting with plasma membrane H^+-ATPase polypeptide (Fig. 8f). This suggests that the plasma membrane H^+-ATPase has been activated at the post-translational level in a manner not affecting the amount of 14-3-3 protein bound considerably.

DISCUSSION

In this work, we demonstrated that infection of *N. benthamiana* plants with PVX can ameliorate defence responses against a subsequent oxidative stress, and attribute this acquired cross-tolerance to differential regulation of plasma membrane Ca^{2+}/H^+ exchangers between control and PVX-inoculated mesophyll cells (as discussed below).

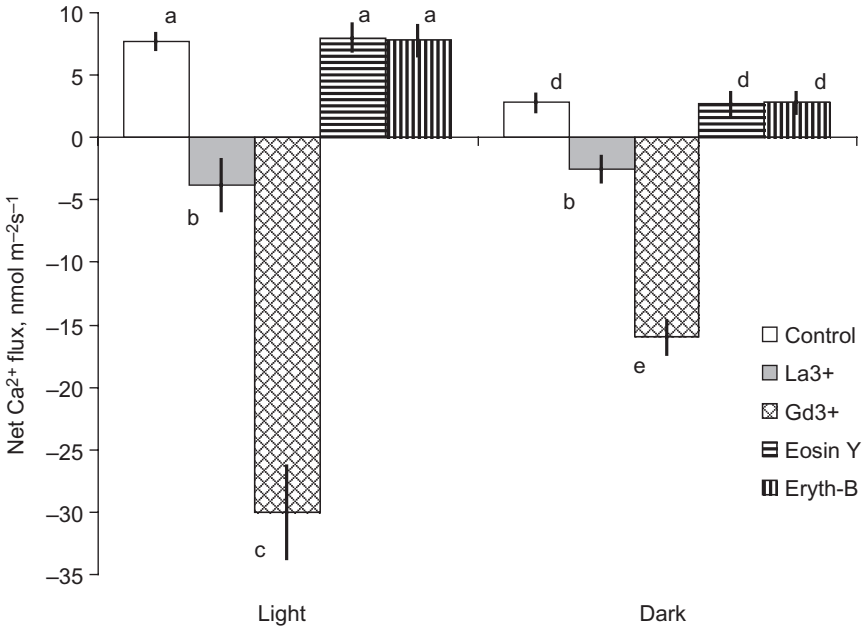

Figure 6. Effect of known blockers of Ca^{2+}-permeable channels (La^{3+}, 1 mM; and Gd^{3+}, 50 μM) and inhibitors of P_{2B}-type ATPase (eosin yellow, 0.5 μM; and erythrocin B, 4 μM) on net Ca^{2+} fluxes in tobacco mesophyll cells. Leaf mesophyll segments were incubated in appropriate concentration of inhibitor for 1–1.5 h prior to measurements. Mean ± SE ($n = 4$ to 6).

Amelioration of detrimental effects of oxidative stress in PVX-inoculated plants

The deleterious effects of UV (mainly UV-B; 290–320 nm) on plants have been extensively studied (Kerr & McElroy 1993; Teramura & Sullivan 1994), and significant impairment of electron transport and a progressive decline in maximum photochemical ability of PSII (Fv/Fm characteristics) were observed (Van Hasselt, Chow & Anderson 1996; Xiong 2001). This is consistent with our observations for UV-C-exposed plants (Fig. 1).

At the ultrastructural level, UV-C stress caused a significant disintegration of the chloroplasts structure (Fig. 2), consistent with other reports for UV-B-treated cells (He, Huang & Whitecross 1994; Yu *et al*. 2005). However, UV stress-induced damage to chloroplast ultrastructure and photosynthetic machinery was much reduced in PVX-inoculated leaves (Figs 1 & 2, respectively). This suggests that tobacco mesophyll cells have acquired an improved resistance to the UV-C stress as a result of their exposure to the PVX virus. As argued below, better control over Ca^{2+} efflux systems may be behind this acquired resistance.

Experiments were also conducted applying H_2O_2 to mesophyll cells from mock controls and PVX-inoculated leaves. In both short- and long-term experiments, PVX-inoculated plants showed a much reduced net Ca^{2+} influx as well as a better K^+ retention ability (Fig. 3). The latter can be considered as a strong evidence for higher oxidative stress tolerance in PVX-inoculated leaves. ROS production is often named as a common denominator in plant stress responses to variety of environmental factors such as salinity, cold, pathogens, UV radiation, ozone, etc. (reviewed in Mittler 2006). At the same time, massive K^+ efflux from plant tissues has been reported in response to all these stresses (e.g. Chen *et al*. 2005, 2007a,b – salt stress; Demidchik *et al*. 2003; Cuin & Shabala 2007; Shabala *et al*. 2007 – oxidative stress; Saltveit 2002 – chilling; Blumwald *et al*. 1998 – pathogens). This efflux may be both a result of ROS-induced lipid peroxidation (Mittler 2006) or direct activation of K^+-permeable plasma membrane channels by ROS (Demidchik *et al*. 2003). Such a massive K^+ leak from the cell reduces the intracellular K^+ pool (Cuin *et al*. 2003) significantly impairing cell metabolism, increasing

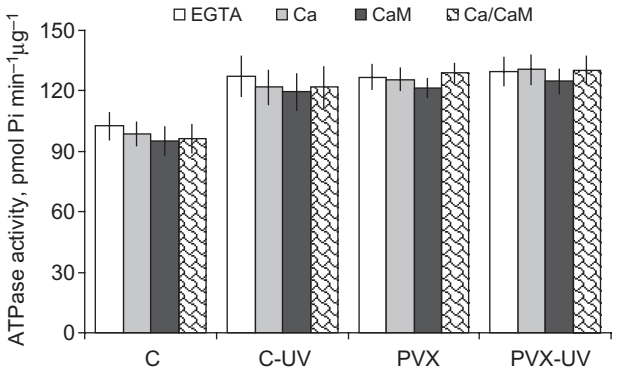

Figure 7. ATP hydrolytic activity of tobacco plasma membranes in absence or presence of Ca^{2+} and CaM, respectively. Measurements were undertaken using purified plasma membranes from tobacco mesophyll tissue in four different buffers: (i) EGTA (free Ca^{2+}); (ii) Ca^{2+} (estimated free Ca^{2+} concentration of 70 μM); (iii) CaM (20 μg mL^{-1}); and (iv) Ca^{2+}/CaM (70 μM-free Ca plus 20 μg mL^{-1} CaM). C, mock control; C-UV, control plants exposed to 20 min of 0.1 J cm^{-2} ultraviolet (UV)-C treatment; PVX, potato virus X (PVX)-inoculated plants; PVX-UV, PVX-inoculated plants exposed to 20 min of 0.1 J cm^{-2} UV-C. Mean ± SE ($n = 4$).

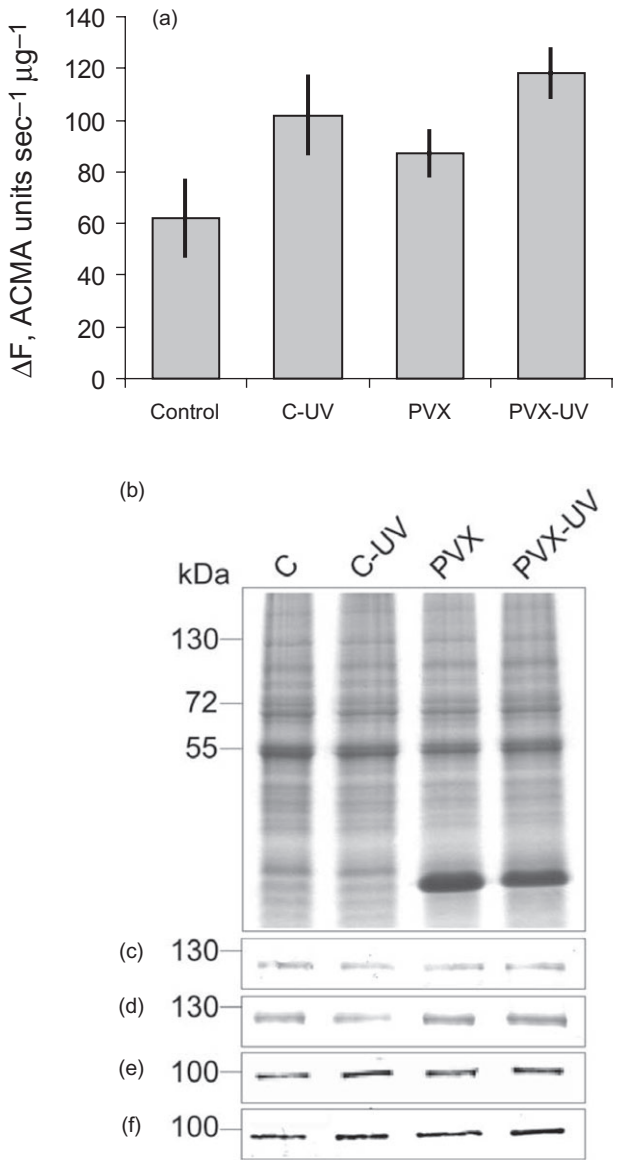

Figure 8. Effect of ultraviolet (UV) treatment on expression and activity of P-type H^+-ATPases (a, e, f) and P_{2B}-type Ca^{2+}-ATPases (c, d) in purified plasma membranes from tobacco leaves (b) exposed to the following treatments: C, mock controls; C-UV, mock controls treated with UV-light (20 min of 0.1 J cm^{-2} UV-C); PVX = potato virus X (PVX)-infected plants; PVX-UV = PVX-inoculated plants treated with UV-light (20 min of 0.1 J cm^{-2} UV-C). (a) Proton pumping measured by the quenching of 9-amino-6-chloro-2-methoxyacridine (ACMA) fluorescence. The experiment shows the initial decrease in fluorescence from three repetitions using 20 μg of the same purification of plasma membranes; (b) Coomassie Brilliant Blue-stained gel; (c) Western blot with a non-isoform-specific polyclonal antibody for P_2B Ca^{2+}-ATPases; (d) CaM overlay assay; (e) Western blot detecting the plasma membrane H^+-ATPase; (f) Far-western analysis showing binding of regulatory 14-3-3 protein to plasma membrane H^+-ATPase. The Western blots, CaM overlay assay and 14-3-3 binding experiments were repeated on two independent plasma membrane purifications.

NADPH-dependent O_2^- generation (Cakmak 2005) and triggering programmed cell death (Huh *et al*. 2002; Shabala 2009). It is therefore not surprising that a plant's ability to retain K^+ in the cell often is correlated with increased stress tolerance (e.g. Chen *et al*. 2005, 2007a,b – salinity; Shamsi *et al*. 2008 – heavy metals; Vicente *et al*. 2006 – heat; Cakmak 2005; Srinivasan, Kumar & Kirti 2009 – oxidative stress). In light of the above, the results shown in Fig. 3 suggest that PVX-inoculated plants possessed higher oxidative stress tolerance, which may explain their better adaptation to UV-C conditions.

Better control over Ca^{2+} efflux systems confers the acquired oxidative stress tolerance

Calcium has been widely implicated as a second messenger in UV-induced oxidative stress. Even millisecond flashes of UV-B radiation are sufficient to raise $[Ca^{2+}]_{cyt}$ and activate expression of some antioxidant enzymes eliminating deleterious ROS molecules (Frohnmeyer, Bowler & Schafer 1997; Frohnmeyer, Grabov & Blatt 1998; Colville & Smirnoff 2008). This is consistent with our results (Fig. 4), where 20 min of UV-C exposure has resulted in prolonged (at least 30 min) statistically significant elevation in $[Ca^{2+}]_{cyt}$. However, PVX-inoculated plants had intrinsically lower $[Ca^{2+}]_{cyt}$ values compared with wild type (WT), and at all times, $[Ca^{2+}]_{cyt}$ values for PVX-inoculated plants were significantly lower than appropriate controls (Fig. 4).

The causal relationship between cytosolic Ca^{2+} levels and oxidative stress tolerance remains to be investigated in detail. On one hand, application of the calcium channel blocker lanthanum reduced H_2O_2-induced $[Ca^{2+}]_{cyt}$ elevation and concomitantly inhibited expression of the glutathione S-transferase 1, a major detoxifying enzyme in plant cells (Rentel & Knight 2004). On the other hand, treatment with H_2O_2 that elicited $[Ca^{2+}]_{cyt}$ increases also brought about a reduction in activity of another key antioxidant enzyme, superoxide dismutase (Price *et al*. 1994). Hence, it appears that while changes in cytosolic-free calcium are important to potentiate antioxidant defence system (Nicotera *et al*. 1985), a fine balance exists between the cytosolic calcium homeostasis and activity of major antioxidants. As shown in this work, PVX-inoculated plants have much better ability to maintain this balance, as is evident from both much quicker activation of the plasma membrane Ca^{2+} efflux systems after UV-light exposure (Fig. 5b) and from direct measurements of cytosolic-free Ca^{2+} using FLIM technique (Fig. 4). Although multiple mechanisms may exist, the plasma membrane NADPH oxidase involvement is most likely. It has been shown before that $[Ca^{2+}]_{cyt}$ activation of NADPH oxidase causes a further rise in $[Ca^{2+}]_{cyt}$ via positive feedback mechanisms (Lecourieux *et al*. 2002). Thus, more active Ca^{2+} removal from the cytosol in PVX-inoculated plants is essential to prevent this activation and maintain ROS levels under control.

The identity of Ca^{2+} efflux systems mediating virus-induced acquired resistance to oxidative stress

Two major types of Ca^{2+} efflux systems are known in plants: Ca^{2+} pumps and Ca^{2+}/H^+ antiporters. These differ significantly in their affinity for calcium (K_m values in the range 0.1–2 mM and 10–15 mM, respectively; Sze *et al*. 2000; White & Broadley 2003). Thus, Ca^{2+} carriers appear to be less selective but more efficient, while Ca^{2+} pumps provide a more precise control over cytosolic Ca^{2+} levels.

Among pumps, only P_{2B}-type Ca^{2+}-ATPases have been shown to be located at the plasma membrane (from which net Ca^{2+} fluxes were measured) (Geisler *et al*. 2000; Axelsen & Palmgren 2001; Bothwell & Ng 2005). The absence of any significant difference in Ca^{2+}-ATPase activity in the purified plasma membranes from tobacco leaves between control and UV-treated plants (Fig. 7), or in the Ca^{2+}-ATPase expression level and its ability to bind CaM in the plasma membrane samples (Fig. 8), suggest that the plasma membrane P_{2B}-type pumps plays no major role in removing excessive Ca^{2+} from the cytosol under oxidative stress conditions. Instead, several lines of evidence implicate plasma membrane Ca^{2+}/H^+ exchangers into oxidative stress responses in our experiments.

Firstly, net Ca^{2+} efflux was measured after cell pretreatment with Gd^{3+} or La^{3+}, two known blockers of Ca^{2+}-permeable channels (Fig. 6), or some time after UV-C exposure (Fig. 5). As passive Ca^{2+} efflux is thermodynamically impossible under the conditions of the experiment, the efflux *must* be mediated by an active Ca^{2+} efflux system. Secondly, the only two types of Ca^{2+} efflux systems known are Ca^{2+}-ATPases and Ca^{2+}/H^+ exchangers (White & Broadley 2003) and, as discussed above, our biochemical assays rule out the involvement of Ca^{2+}-ATPases. Thirdly, neither EY nor EB, two known P_{2B}-type Ca^{2+}-ATPase inhibitors (Bush 1995; Beffagna *et al*. 2005), affected net Ca^{2+} fluxes (Fig. 6) suggesting that plasma membrane P_{2B}-type Ca^{2+}-ATPases play no major role in mediating Ca^{2+} flux across the plasma membrane. Finally, both UV light and PVX infection caused additive increases in plasma membrane H^+-ATPase-catalysed proton pumping (Fig. 8a). Thus, these stresses cause an increase in the electrochemical proton gradient that serve as the energy source for co-transport systems such as plasma membrane Ca^{2+}/H^+ exchangers. Taken together, these results strongly suggest that a Ca^{2+}/H^+ exchanger mediates the observed Ca^{2+} efflux, but direct evidence for this hypothesis remains to be presented.

Ca^{2+}/H^+ antiporter activity is best characterized for the tonoplast (Sanders *et al*. 1999; Hirschi 2001). Although no direct evidence was presented at the molecular level, most authors agree that such transporters also operate at the plasma membrane (Kasai & Muto 1990; Sanders *et al*. 1999; White & Broadley 2003). Our data reported here provide an additional support for this idea providing electrophysiological evidence for the presence of such Ca^{2+}/H^+ exchangers at the plasma membrane in tobacco mesophyll cells.

Our findings also reopen an interesting debate on whether viral pathogenesis may be beneficial to plants under certain conditions (Fraser 1992; Xu *et al*. 2008). The beneficial role of viruses in plant hosts is rarely addressed in the literature. Meanwhile, in the field conditions, co-occurrence of a variety of different stresses is common, and a possibility of viral-enhanced abiotic stress tolerance could be of significant agricultural importance.

ACKNOWLEDGMENTS

This work was supported by the ARC Discovery and TIAR grants (S.S.), the USDA/ARS (L.G.N.), the EU Framework Programme 6 (PHIME) and by the Danish National Research Foundation. We are grateful to C. Murphy from BARC Electron Microscopy Unit for his invaluable help with tissue preparation and taking EM images, to J. C. Dickens of the Insect Behaviour Laboratory and J. Bunce of the Crop Systems and Global Change Laboratory, USDA/ARS for sharing their equipment.

REFERENCES

AbuQamar S., Luo H.L., Laluk K., Mickelbart M.V. & Mengiste T. (2009) Crosstalk between biotic and abiotic stress responses in tomato is mediated by the AIM1 transcription factor. *The Plant Journal* **58,** 347–360.

Apel K. & Hirt H. (2004) Reactive oxygen species: metabolism, oxidative stress, and signal transduction. *Annual Review of Plant Biology* **55,** 373–399.

Axelsen K.B. & Palmgren M.G. (2001) Inventory of the superfamily of P-type ion pumps in *Arabidopsis*. *Plant Physiology* **126,** 696–706.

Bækgaard L., Luoni L., De Michelis M.I. & Palmgren M.G. (2006) The plant plasma membrane Ca^{2+} pump ACA8 contains overlapping as well as physically separated autoinhibitory and calmodulin-binding domains. *The Journal of Biological Chemistry* **281,** 1058–1065.

Beffagna N., Buffoli B. & Busi C. (2005) Modulation of reactive oxygen species production during osmotic stress in *Arabidopsis thaliana* cultured cells: involvement of the plasma membrane Ca^{2+}-ATPase and H^+-ATPase. *Plant and Cell Physiology* **46,** 1326–1339.

Blume B., Nürnberger T., Nass N. & Scheel D. (2000) Receptor-mediated increase in cytoplasmic free calcium required for activation of pathogen defense in parsley. *The Plant Cell* **12,** 1425–1440.

Blumwald E., Aharon G.S. & Lam C.H. (1998) Early signal transduction pathways in plant–pathogen interactions. *Trends in Plant Science* **3,** 342–346.

Bostock R.M. (2005) Signal crosstalk and induced resistance: straddling the line between cost and benefit. *Annual Review of Phytopathology* **43,** 545–580.

Bothwell J.H.F. & Ng C.K.Y. (2005) The evolution of Ca^{2+} signalling in photosynthetic eukaryotes. *New Phytologist* **166,** 21–38.

Bowler C. & Fluhr R. (2000) The role of calcium and activated oxygens as signals for controlling cross-tolerance. *Trends in Plant Science* **5,** 241–246.

Bradford M.M. (1976) Rapid and sensitive method for quantification of microgram quantities of protein utilizing principle of protein-dye binding. *Analytical Biochemistry* **72,** 248–254.

Bush D.S. (1995) Calcium regulation in plant cells and its role in signaling. *Annual Review of Plant Physiology and Plant Molecular Biology* **46,** 95–122.

Cakmak I. (2005) The role of potassium in alleviating detrimental effects of abiotic stresses in plants. *Journal of Plant Nutrition and Soil Science* **168,** 521–530.

Capiati D.A., Pais S.M. & Tellez-Inon M.T. (2006) Wounding increases salt tolerance in tomato plants: evidence on the participation of calmodulin-like activities in cross-tolerance signalling. *Journal of Experimental Botany* **57,** 2391–2400.

Chen Z., Newman I., Zhou M., Mendham N., Zhang G. & Shabala S. (2005) Screening plants for salt tolerance by measuring K^+ flux: a case study for barley. *Plant, Cell & Environment* **28,** 1230–1246.

Chen Z.H., Pottosin I.I., Cuin T.A., *et al*. (2007a) Root plasma membrane transporters controlling K^+/Na^+ homeostasis in salt-stressed barley. *Plant Physiology* **145,** 1714–1725.

Chen Z.H., Zhou M.X., Newman I.A., Mendham N.J., Zhang G.P. & Shabala S. (2007b) Potassium and sodium relations in salinised barley tissues as a basis of differential salt tolerance. *Functional Plant Biology* **34,** 150–162.

Colville L. & Smirnoff N. (2008) Antioxidant status, peroxidase activity, and PR protein transcript levels in ascorbate-deficient *Arabidopsis thaliana vtc* mutants. *Journal of Experimental Botany* **59,** 3857–3868.

Cuin T.A. & Shabala S. (2007) Compatible solutes reduce ROS-induced potassium efflux in *Arabidopsis* roots. *Plant, Cell & Environment* **30,** 875–885.

Cuin T.A., Miller A.J., Laurie S.A. & Leigh R.A. (2003) Potassium activities in cell compartments of salt-grown barley leaves. *Journal of Experimental Botany* **54,** 657–661.

Demidchik V., Shabala S.N., Coutts K.B., Tester M.A. & Davies J.M. (2003) Free oxygen radicals regulate plasma membrane Ca^{2+} and K^+- permeable channels in plant root cells. *Journal of Cell Science* **116,** 81–88.

Demidchik V., Shabala S.N. & Davies J.M. (2007) Spatial variation in H_2O_2 response of *Arabidopsis thaliana* root epidermal Ca^{2+} flux and plasma membrane Ca^{2+} channels. *The Plant Journal* **49,** 377–386.

Dempsey D.A., Shah J. & Klessig D.F. (1999) Salicylic acid and disease resistance in plants. *Critical Review in Plant Science* **18,** 547–575.

Fraser R.S.S. (1992) Plant viruses as agents to modify the plant phenotype for good or evil. In *Genetic Engineering with Plant Viruses* (eds T.M.A. Wilson & J. Davies) pp. 1–23. CRC Press Inc., Boca Raton, FL, USA.

Frohnmeyer H., Bowler C. & Schafer E. (1997) Evidence for some signal transduction elements involved in UV-light-dependent responses in parsley protoplasts. *Journal of Experimental Botany* **48,** 739–750.

Frohnmeyer H., Grabov A. & Blatt M.R. (1998) A role for the vacuole in auxin-mediated control of cytosolic pH by *Vicia* mesophyll and guard cells. *The Plant Journal* **13,** 109–116.

Fuglsang A.T., Visconti S., Drumm K., Jahn T., Stensballe A., Mattei B., Jensen O.N., Aducci P. & Palmgren M.G. (1999) Binding of 14-3-3 protein to the plasma membrane H^+-ATPase AHA2 involves the three C-terminal residues Tyr946-Thr-Val and requires phosphorylation of Thr947. *The Journal of Biological Chemistry* **274,** 36774–36780.

Geisler M., Axelsen K.B., Harper J.F. & Palmgren M.G. (2000) Molecular aspects of higher plant P-type Ca^{2+}-ATPases. *Biochimica et Biophysica Acta* **1465,** 52–78.

Guo K.-M., Babourina O. & Rengel Z. (2009) Na^+/H^+ antiporter activity of the SOS1 gene: lifetime imaging analysis and electrophysiological studies on *Arabidopsis* seedlings. *Physiologia Plantarum* **137,** 155–165.

He J., Huang L.K. & Whitecross M.I. (1994) Chloroplast ultrastructure changes in *Pisum sativum* associated with supplementary ultraviolet (UV-B) radiation. *Plant, Cell & Environment* **17,** 771–775.

Hepler P.K. & Wayne R.O. (1985) Calcium and plant development. *Annual Review of Plant Physiology and Plant Molecular Biology* **36,** 397–439.

Hetherington A.M. & Brownlee C. (2004) The generation of Ca^{2+} signals in plants. *Annual Review of Plant Biology Biology* **55,** 401–427.

Hirschi K. (2001) Vacuolar H^+/Ca^{2+} transport: who's directing the traffic? *Trends in Plant Science* **6,** 100–104.

Hu X.L., Jiang M.Y., Zhang J.H., Zhang A.Y., Lin F. & Tan M.P. (2007) Calcium-calmodulin is required for abscisic acid-induced antioxidant defense and functions both upstream and downstream of H_2O_2 production in leaves of maize (*Zea mays*) plants. *New Phytologist* **173,** 27–38.

Huh G.H., Damsz B., Matsumoto T.K., Reddy M.P., Rus A.M., Ibeas J.I., Narasimhan M.L., Bressan R.A. & Hasegawa P.M. (2002) Salt causes ion disequilibrium-induced programmed cell death in yeast and plants. *The Plant Journal* **29,** 649–659.

Jornot L., Maechler P., Wollheim C.B. & Junod A.F. (1999) Reactive oxygen metabolites increase mitochondrial calcium in endothelial cells: implication of the Ca^{2+}/Na^+ exchanger. *Journal of Cell Science* **112,** 1013–1022.

Kasai M. & Muto S. (1990) Ca^{2+} pump and Ca^{2+}/H^+ antiporter in plasma-membrane vesicles isolated by aqueous 2-phase partitioning from corn leaves. *The Journal of Membrane Biology* **114,** 133–142.

Kerr J.B. & McElroy C.T. (1993) Evidence for large upward trends of ultraviolet-B radiation linked to ozone depletion. *Science* **262,** 1032–1034.

Laemmli U.K. (1970) Cleavage of structural proteins during assembly of head of bacteriophageT4. *Nature* **227,** 680–685.

Larsson C., Widell S. & Kjellbom P. (1987) Preparation of high purity plasma membranes. *Methods in Enzymology* **148,** 568–588.

Lecourieux D., Mazars C., Pauly N., Ranjeva R. & Pugin A. (2002) Analysis and effects of cytosolic free calcium increases in response to elicitors in *Nicotiana plumbaginifolia* cells. *The Plant Cell* **14,** 2627–2641.

Mittler R. (2006) Abiotic stress, the field environment and stress combination. *Trends in Plant Science* **11,** 15–19.

Mori I.C. & Schroeder J.I. (2004) Reactive oxygen species activation of plant Ca^{2+} channels. A signaling mechanism in polar growth, hormone transduction, stress signaling, and hypothetically mechanotransduction. *Plant Physiology* **135,** 702–708.

Nemchinov L.G., Shabala L. & Shabala S. (2008) Calcium efflux as a component of the hypersensitive response of *Nicotiana benthamiana* to *Pseudomonas syringae*. *Plant and Cell Physiology* **49,** 40–46.

Nicotera P., Moore M., Mirabelli F., Bellomo G. & Orrenius S. (1985) Inhibition of hepatocyte plasma-membrane Ca^{2+}-ATPase activity by menadione metabolism and its restoration by thiols. *FEBS Letters* **181,** 149–153.

Niittyla T., Fuglsang A.T., Palmgren M.G., Frommer W.B. & Schulze W.X. (2007) Temporal analysis of sucrose-induced phosphorylation changes in plasma membrane proteins of arabidopsis. *Molecular & Cellular Proteomics* **6,** 1711–1726.

Nürnberger T., Nennstiel D., Jabs T., Sacks W.R., Hahlbrock K. & Scheel D. (1994) High affinity binding of a fungal oligopeptide elicitor to parsley plasma membranes triggers multiple defense responses. *Cell* **78,** 449–460.

Palmgren M.G. (2001) Plant plasma membrane H^+-ATPases: powerhouses for nutrient uptake. *Annual Review of Plant Physiology and Plant Molecular Biology* **52,** 817–845.

Pang C.-H. & Wang B.-S. (2008) Oxidative stress and salt tolerance in plants. *Progress in Botany* **69,** 231–245.

Patton C., Thompson S. & Epel D. (2004) Some precautions in using chelators to buffer metals in biological solutions. *Cell Calcium* **35,** 427–431.

Pei Z.M., Murata Y., Benning G., Thomine S., Klusener B., Allen G.J., Grill E. & Schroeder J.I. (2000) Calcium channels activated by hydrogen peroxide mediate abscisic acid signalling in guard cells. *Nature* **406,** 731–734.

Price A.H., Taylor A., Ripley S.J., Griffiths A., Trewavas A.J. & Knight M.R. (1994) Oxidative signals in tobacco increase cytosolic calcium. *The Plant Cell* **6,** 1301–1310.

Remacle J., Raes M., Toussaint O., Renard P. & Rao G. (1995) Low levels of reactive oxygen species as modulators of cell function. *Mutation Research* **316,** 103–122.

Rentel M.C. & Knight M.R. (2004) Oxidative stress-induced calcium signaling in *Arabidopsis*. *Plant Physiology* **135,** 1471–1479.

Romani G., Bonza M.C., Filippini I., Cerana M., Beffagna N. & De Michelis M.I. (2004) Involvement of the plasma membrane Ca^{2+}-ATPase in the short-term response of *Arabidopsis thaliana* cultured cells to oligogalacturonides. *Plant Biology* **6,** 192–200.

Sabehat A., Weiss D. & Lurie S. (1998) Heat-shock proteins and cross-tolerance in plants. *Physiologia Plantarum* **103,** 437–441.

Saltveit M.E. (2002) The rate of ion leakage from chilling-sensitive tissue does not immediately increase upon exposure to chilling temperatures. *Postharvest Biology and Technology* **26,** 295–304.

Sanders D., Brownlee C. & Harper J.F. (1999) Communicating with calcium. *The Plant Cell* **11,** 691–706.

Schiøtt M., Romanowsky S.M., Bækgaard L., Jakobsen M.K., Palmgren M.G. & Harper J.F. (2004) A plant plasma membrane Ca^{2+} pump is required for normal pollen tube growth and fertilization. *Proceedings of the National Academy of Sciences of the United States of America* **101,** 9502–9507.

Shabala S. (2009) Salinity and programmed cell death: unravelling mechanisms for ion specific signalling. *Journal of Experimental Botany* **60,** 709–711.

Shabala S. & Newman I. (2000) Salinity effects on the activity of plasma membrane H^+ and Ca^{2+} transporters in bean leaf mesophyll: masking role of the cell wall. *Annals of Botany* **85,** 681–686.

Shabala S., Babourina O.K. & Newman I.A. (2000) Ion-specific mechanisms of osmoregulation in bean mesophyll cells. *Journal of Experimental Botany* **51,** 1243–1253.

Shabala L., Ross T., McMeekin T. & Shabala S. (2006a) Non-invasive microelectrode ion flux measurements to study adaptive responses of microorganisms to the environment. *FEMS Microbiology Reviews* **30,** 472–486.

Shabala S., Demidchik V., Shabala L., Cuin T.A., Smith S.J., Miller A.J., Davies J.M. & Newman I.A. (2006b) Extracellular Ca^{2+} ameliorates NaCl-induced K^+ loss from *Arabidopsis* root and leaf cells by controlling plasma membrane K^+permeable channels. *Plant Physiology* **141,** 1653–1665.

Shabala S., Cuin T.A., Prismall L. & Nemchinov L.G. (2007) Expression of animal CED-9 anti-apoptotic gene in tobacco modifies plasma membrane ion fluxes in response to salinity and oxidative stress. *Planta* **227,** 189–197.

Shamsi I.H., Jilani G., Zhang G.P. & Wei K. (2008) Cadmium stress tolerance through potassium nutrition in soybean. *Asian Journal of Chemistry* **20,** 1099–1108.

Sharma Y.K., Leont J., Raskin I. & Davis K.R. (1996) Ozone-induced responses in *Arabidopsis thaliana*: the role of salicylic acid in the accumulation of defense-related transcripts and induced resistance. *Proceedings of the National Academy of Sciences of the United States of America* **93,** 5099–5104.

Srinivasan T., Kumar K.R.R. & Kirti P.B. (2009) Constitutive expression of a trypsin protease inhibitor confers multiple stress tolerance in transgenic tobacco. *Plant and Cell Physiology* **50,** 541–553.

Sze H., Liang F., Hwang I., Curran A.C. & Harper J.F. (2000) Diversity and regulation of plant Ca^{2+} pumps: insights from expression in yeast. *Annual Review of Plant Physiology and Plant Molecular Biology* **51,** 433–462.

Teramura A.H. & Sullivan J.H. (1994) Effects of UV-B radiation on photosynthesis and growth of terrestrial plants. *Photosynthesis Research* **39,** 463–473.

Van Hasselt P.R., Chow W.S. & Anderson J.M. (1996) Short-term treatment of pea leaves with supplementary UV-B at different oxygen concentrations: impacts on chloroplast and plasma membrane bound processes. *Plant Science* **120,** 1–9.

Vicente A.R., Martinez G.A., Chaves A.R. & Civello P.M. (2006) Effect of heat treatment on strawberry fruit damage and oxidative metabolism during storage. *Postharvest Biology and Technology* **40,** 116–122.

White P.J. & Broadley M.R. (2003) Calcium in plants. *Annals of Botany* **92,** 487–511.

Xiong F.S. (2001) Evidence that UV-B tolerance of the photosynthetic apparatus in microalgae is related to the D1-turnover mediated repair cycle in vivo. *Journal of Plant Physiology* **158,** 285–294.

Xu P., Chen F., Mannas J.P., Feldman T., Sumner L.W. & Roossinck M.J. (2008) Virus infection improves drought tolerance. *New Phytologist* **180,** 911–921.

Yalpani N., Enyedi A.J., Leon J. & Raskin I. (1994) Ultraviolet light and ozone stimulate accumulation of salicylic acid, pathogenesis-related proteins and virus resistance in tobacco. *Planta* **193,** 372–376.

Yu J., Tang X.X., Zhang P.Y., Tian J.Y. & Dong S.L. (2005) Physiological and ultrastructural changes of *Chlorella sp* induced by UV-B radiation. *Progress in Natural Science* **15,** 678–683.

Zaidi A. & Michaelis M.L. (1999) Effects of reactive oxygen species on brain synaptic plasma membrane Ca^{2+}-ATPase. *Free Radical Biology and Medicine* **27,** 810–821.

Received 13 July 2010; received in revised form 12 October 2010; accepted for publication 19 October 2010

SUPPORTING INFORMATION

Additional Supporting Information may be found in the online version of this article:

Figure S1. Effect of potato virus X (PVX) inoculation on growth and phenology of *Nicotiana benthamiana* plants. Plants were inoculated at 3 weeks. (a, b) Mock control (a) and PVX-inoculated plant (b) 10 d post-inoculation. (c, d) mock control (c) and PVX-inoculated plant (d) 25 d post-inoculation.

Please note: Wiley-Blackwell are not responsible for the content or functionality of any supporting materials supplied by the authors. Any queries (other than missing material) should be directed to the corresponding author for the article.